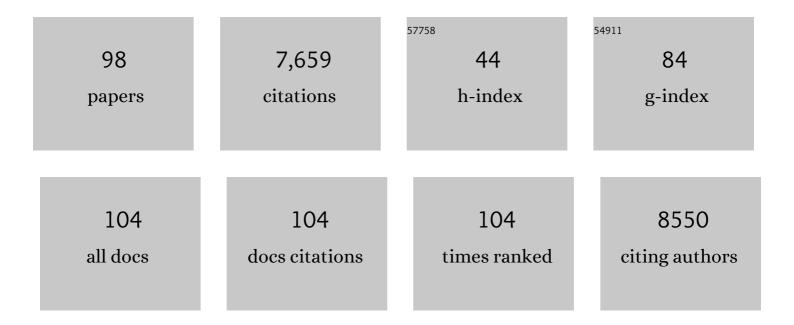
## **James Sharpe**

List of Publications by Year in descending order

Source: https://exaly.com/author-pdf/2200164/publications.pdf Version: 2024-02-01



INMES SHADDE

#	Article	IF	CITATIONS
1	Optical Projection Tomography as a Tool for 3D Microscopy and Gene Expression Studies. Science, 2002, 296, 541-545.	12.6	1,129
2	Senescence Is a Developmental Mechanism that Contributes to Embryonic Growth and Patterning. Cell, 2013, 155, 1119-1130.	28.9	898
3	Positional information and reaction-diffusion: two big ideas in developmental biology combine. Development (Cambridge), 2015, 142, 1203-1211.	2.5	317
4	<i>Hox</i> Genes Regulate Digit Patterning by Controlling the Wavelength of a Turing-Type Mechanism. Science, 2012, 338, 1476-1480.	12.6	309
5	Reprogramming Hox Expression in the Vertebrate Hindbrain: Influence of Paraxial Mesoderm and Rhombomere Transposition. Neuron, 1996, 16, 487-500.	8.1	189
6	Tomographic molecular imaging and 3D quantification within adult mouse organs. Nature Methods, 2007, 4, 31-33.	19.0	178
7	The Role of Spatially Controlled Cell Proliferation in Limb Bud Morphogenesis. PLoS Biology, 2010, 8, e1000420.	5.6	175
8	Optical Projection Tomography. Annual Review of Biomedical Engineering, 2004, 6, 209-228.	12.3	174
9	Optical projection tomography as a new tool for studying embryo anatomy. Journal of Anatomy, 2003, 202, 175-181.	1.5	156
10	An atlas of gene regulatory networks reveals multiple threeâ€gene mechanisms for interpreting morphogen gradients. Molecular Systems Biology, 2010, 6, 425.	7.2	153
11	Mechanobiology of embryonic skeletal development: Insights from animal models. Birth Defects Research Part C: Embryo Today Reviews, 2010, 90, 203-213.	3.6	134
12	A unified design space of synthetic stripe-forming networks. Nature Communications, 2014, 5, 4905.	12.8	128
13	Visualizing Plant Development and Gene Expression in Three Dimensions Using Optical Projection Tomography. Plant Cell, 2006, 18, 2145-2156.	6.6	127
14	Identification of Sonic hedgehog as a candidate gene responsible for the polydactylous mouse mutant Sasquatch. Current Biology, 1999, 9, 97-S1.	3.9	125
15	Perspective: The promise of multi-cellular engineered living systems. APL Bioengineering, 2018, 2, 040901.	6.2	110
16	EMAP and EMAGE: A Framework for Understanding Spatially Organized Data. Neuroinformatics, 2003, 1, 309-326.	2.8	109
17	High-throughput mathematical analysis identifies Turing networks for patterning with equally diffusing signals. ELife, 2016, 5, .	6.0	108
18	pMHC affinity controls duration of CD8+ T cell–DC interactions and imprints timing of effector differentiation versus expansion. Journal of Experimental Medicine, 2016, 213, 2811-2829.	8.5	101

#	Article	IF	CITATIONS
19	Correction of artefacts in optical projection tomography. Physics in Medicine and Biology, 2005, 50, 4645-4665.	3.0	99
20	Decrease in Cell Volume Generates Contractile Forces Driving Dorsal Closure. Developmental Cell, 2015, 33, 611-621.	7.0	99
21	Resolution improvement in emission optical projection tomography. Physics in Medicine and Biology, 2007, 52, 2775-2790.	3.0	95
22	In vitro whole-organ imaging: 4D quantification of growing mouse limb buds. Nature Methods, 2008, 5, 609-612.	19.0	95
23	Quantification and Three-Dimensional Imaging of the Insulitis-Induced Destruction of Î <sup>2</sup> -Cells in Murine Type 1 Diabetes. Diabetes, 2010, 59, 1756-1764.	0.6	88
24	Turing patterns in development: what about the horse part?. Current Opinion in Genetics and Development, 2012, 22, 578-584.	3.3	87
25	3D representation of Wnt and Frizzled gene expression patterns in the mouse embryo at embryonic day 11.5 (Ts19). Gene Expression Patterns, 2008, 8, 331-348.	0.8	84
26	Image formation by linear and nonlinear digital scanned light-sheet fluorescence microscopy with Gaussian and Bessel beam profiles. Biomedical Optics Express, 2012, 3, 1492.	2.9	83
27	The fin-to-limb transition as the re-organization of a Turing pattern. Nature Communications, 2016, 7, 11582.	12.8	80
28	A Local, Self-Organizing Reaction-Diffusion Model Can Explain Somite Patterning in Embryos. Cell Systems, 2015, 1, 257-269.	6.2	79
29	Computer modeling in developmental biology: growing today, essential tomorrow. Development (Cambridge), 2017, 144, 4214-4225.	2.5	78
30	3 dimensional modelling of early human brain development using optical projection tomography. BMC Neuroscience, 2004, 5, 27.	1.9	69
31	Spleen versus pancreas: strict control of organ interrelationship revealed by analyses of Bapx1-/- mice. Genes and Development, 2006, 20, 2208-2213.	5.9	68
32	Three-Dimensional Imaging of Drosophila melanogaster. PLoS ONE, 2007, 2, e834.	2.5	66
33	Scapula development is governed by genetic interactions of <i>Pbx1</i> with its family members and with <i>Emx2</i> via their cooperative control of <i>Alx1</i> . Development (Cambridge), 2010, 137, 2559-2569.	2.5	65
34	Cell tracing reveals a dorsoventral lineage restriction plane in the mouse limb bud mesenchyme. Development (Cambridge), 2007, 134, 3713-3722.	2.5	64
35	Fluorescence lifetime optical projection tomography. Journal of Biophotonics, 2008, 1, 390-394.	2.3	62
36	A spectrum of modularity in multiâ€functional gene circuits. Molecular Systems Biology, 2017, 13, 925.	7.2	62

#	Article	IF	CITATIONS
37	Salivary gland macrophages and tissue-resident CD8 <sup>+</sup> T cells cooperate for homeostatic organ surveillance. Science Immunology, 2020, 5, .	11.9	57
38	FishNet: an online database of zebrafish anatomy. BMC Biology, 2007, 5, 34.	3.8	56
39	Immobilized chicks as a model system for earlyâ€onset developmental dysplasia of the hip. Journal of Orthopaedic Research, 2014, 32, 777-785.	2.3	56
40	Live optical projection tomography. Organogenesis, 2009, 5, 211-216.	1.2	49
41	4D retrospective lineage tracing using SPIM for zebrafish organogenesis studies. Journal of Biophotonics, 2011, 4, 122-134.	2.3	49
42	Evidence that Fgf10 contributes to the skeletal and visceral defects of an apert syndrome mouse model. Developmental Dynamics, 2009, 238, 376-385.	1.8	48
43	Joint shape morphogenesis precedes cavitation of the developing hip joint. Journal of Anatomy, 2014, 224, 482-489.	1.5	48
44	High-resolution three-dimensional imaging of islet-infiltrate interactions based on optical projection tomography assessments of the intact adult mouse pancreas. Journal of Biomedical Optics, 2008, 13, 1.	2.6	46
45	Budding behaviors: Growth of the limb as a model of morphogenesis. Developmental Dynamics, 2011, 240, 1054-1062.	1.8	46
46	<i>N-myc</i> Controls Proliferation, Morphogenesis, and Patterning of the Inner Ear. Journal of Neuroscience, 2011, 31, 7178-7189.	3.6	46
47	A shift in anterior–posterior positional information underlies the fin-to-limb evolution. ELife, 2015, 4,	6.0	46
48	Image Processing Assisted Algorithms for Optical Projection Tomography. IEEE Transactions on Medical Imaging, 2012, 31, 1-15.	8.9	45
49	OPTiSPIM: integrating optical projection tomography in light sheet microscopy extends specimen characterization to nonfluorescent contrasts. Optics Letters, 2014, 39, 1053.	3.3	44
50	3D confocal reconstruction of gene expression in mouse. Mechanisms of Development, 2001, 100, 59-63.	1.7	43
51	Localization and fate of Fgf10-expressing cells in the adult mouse brain implicate Fgf10 in control of neurogenesis. Molecular and Cellular Neurosciences, 2008, 37, 857-868.	2.2	43
52	Dynamics of gene circuits shapes evolvability. Proceedings of the National Academy of Sciences of the United States of America, 2015, 112, 2103-2108.	7.1	42
53	Genetic background influences embryonic lethality and the occurrence of neural tube defects in Men1 null mice: relevance to genetic modifiers. Journal of Endocrinology, 2009, 203, 133-142.	2.6	38
54	Near Infrared Optical Projection Tomography for Assessments of β-cell Mass Distribution in Diabetes Research. Journal of Visualized Experiments, 2013, , e50238.	0.3	37

#	Article	IF	CITATIONS
55	Clonal Analysis in Mice Underlines the Importance of Rhombomeric Boundaries in Cell Movement Restriction during Hindbrain Segmentation. PLoS ONE, 2010, 5, e10112.	2.5	37
56	A landmark-free morphometric staging system for the mouse limb bud. Development (Cambridge), 2011, 138, 1227-1234.	2.5	36
57	Dataâ€driven modelling of a gene regulatory network for cell fate decisions in the growing limbÂbud. Molecular Systems Biology, 2015, 11, 815.	7.2	36
58	A GDF5 Point Mutation Strikes Twice - Causing BDA1 and SYNS2. PLoS Genetics, 2013, 9, e1003846.	3.5	34
59	Synthetic circuits reveal how mechanisms of gene regulatory networks constrain evolution. Molecular Systems Biology, 2018, 14, e8102.	7.2	34
60	ya  a: GPU-Powered Spheroid Models for Mesenchyme and Epithelium. Cell Systems, 2019, 8, 261-266.e3.	6.2	33
61	Control of pelvic girdle development by genes of the Pbx family and <i>Emx2</i> . Developmental Dynamics, 2011, 240, 1173-1189.	1.8	32
62	A Computational Clonal Analysis of the Developing Mouse Limb Bud. PLoS Computational Biology, 2011, 7, e1001071.	3.2	32
63	A global "imaging'' view on systems approaches in immunology. European Journal of Immunology, 201 42, 3116-3125.	.2. 2.9	32
64	Naive B-cell trafficking is shaped by local chemokine availability and LFA-1–independent stromal interactions. Blood, 2013, 121, 4101-4109.	1.4	32
65	Wolpert's French Flag: what's the problem?. Development (Cambridge), 2019, 146, .	2.5	31
66	Optical Projection Tomography of Vertebrate Embryo Development. Cold Spring Harbor Protocols, 2011, 2011, pdb.top116.	0.3	27
67	Light sheet fluorescence microscopy for in situ cell interaction analysis in mouse lymph nodes. Journal of Immunological Methods, 2016, 431, 1-10.	1.4	27
68	3D modelling, gene expression mapping and post-mapping image analysis in the developing human brain. Brain Research Bulletin, 2005, 66, 449-453.	3.0	26
69	On the concept of mechanism in development. , 2014, , 56-78.		26
70	Preparation of Mouse Embryos for Optical Projection Tomography Imaging. Cold Spring Harbor Protocols, 2011, 2011, pdb.prot5639-pdb.prot5639.	0.3	23
71	The Rho regulator Myosin IXb enables nonlymphoid tissue seeding of protective CD8+ T cells. Journal of Experimental Medicine, 2018, 215, 1869-1890.	8.5	22
72	Topologically selective islet vulnerability and self-sustained downregulation of markers for β-cell maturity in streptozotocin-induced diabetes. Communications Biology, 2020, 3, 541.	4.4	22

#	Article	IF	CITATIONS
73	Antigen Availability and DOCK2-Driven Motility Govern CD4+ T Cell Interactions with Dendritic Cells In Vivo. Journal of Immunology, 2017, 199, 520-530.	0.8	21
74	Migratory appendicular muscles precursor cells in the common ancestor to all vertebrates. Nature Ecology and Evolution, 2017, 1, 1731-1736.	7.8	21
75	Attenuation artifacts in light sheet fluorescence microscopy corrected by OPTiSPIM. Light: Science and Applications, 2018, 7, 70.	16.6	21
76	Design principles of stripe-forming motifs: the role of positive feedback. Scientific Reports, 2014, 4, 5003.	3.3	20
77	Intravital imaging of hair-cell development and regeneration in the zebrafish. Frontiers in Neuroanatomy, 2013, 7, 33.	1.7	17
78	Quantitative Measurements in 3-Dimensional Datasets of Mouse Lymph Nodes Resolve Organ-Wide Functional Dependencies. Computational and Mathematical Methods in Medicine, 2012, 2012, 1-8.	1.3	16
79	A quantitative method for staging mouse embryos based on limb morphometry. Development (Cambridge), 2018, 145, .	2.5	16
80	Gene expression analysis of canonical Wnt pathway transcriptional regulators during early morphogenesis of the facial region in the mouse embryo. Gene Expression Patterns, 2009, 9, 296-305.	0.8	14
81	ESCRT-II/Vps25 Constrains Digit Number by Endosome-Mediated Selective Modulation of FGF-SHH Signaling. Cell Reports, 2014, 9, 674-687.	6.4	12
82	Geometric Morphometrics on Gene Expression Patterns Within Phenotypes: A Case Example on Limb Development. Systematic Biology, 2016, 65, 194-211.	5.6	12
83	Quantification of gene expression patterns to reveal the origins of abnormal morphogenesis. ELife, 2018, 7, .	6.0	12
84	Mechanistic Explanations for Restricted Evolutionary Paths That Emerge from Gene Regulatory Networks. PLoS ONE, 2013, 8, e61178.	2.5	11
85	Toward Controllable Morphogenesis in Large Robot Swarms. IEEE Robotics and Automation Letters, 2019, 4, 3386-3393.	5.1	9
86	Arrested coalescence of multicellular aggregates. Soft Matter, 2022, 18, 3771-3780.	2.7	9
87	Two ways to use imaging: focusing directly on mechanism, or indirectly via behaviour?. Current Opinion in Genetics and Development, 2011, 21, 523-529.	3.3	6
88	$\hat{l}$ ¼Match: 3D Shape Correspondence for Biological Image Data. Frontiers in Computer Science, 2022, 4, .	2.8	6
89	ViceCT and whiceCT for simultaneous high-resolution visualization of craniofacial, brain and ventricular anatomy from micro-computed tomography. Scientific Reports, 2020, 10, 18772.	3.3	4

90 Optical Projection Tomography. , 2009, , 199-224.

#	Article	IF	CITATIONS
91	In-silico organogenesis: Image-driven modelling of limb development. , 2012, , .		1
92	Other Organs. , 0, , 311-332.		0
93	Cells unite by trapping a signal. Nature, 2014, 515, 41-42.	27.8	Ο
94	Sequences Generated by Powers of the <i>k</i> th-order Fibonacci Recurrence Relation. American Mathematical Monthly, 2018, 125, 443-446.	0.3	0
95	Novel Techniques for 3D Biological Microscopy. , 2007, , .		0
96	Inâ€silico organogenesis: measuring and modelling vertebrate limb development. FASEB Journal, 2012, 26, 337.3.	0.5	0
97	ya  a: GPU-powered Spheroid Models for Mesenchyme and Epithelium. SSRN Electronic Journal, 0, , .	0.4	0
98	Dose dependent effects of green tea extracts in the skeletal development of a Down syndrome mouse model. FASEB Journal, 2022, 36, .	0.5	0